Biotechnology Reports 30 (2021) e00621

Contents lists available at ScienceDirect

Biotechnology Reports

journal homepage: www.elsevier.com/locate/btre

Identification, characterization, and lipid profiling of microalgae *Scenedesmus* sp. NC1, isolated from coal mine effluent with potential for biofuel production

Niwas Kumar[b], Chiranjib Banerjee[a,*], Sheeja Jagadevan[b]

[a] Department of Botany & Microbiology (Deemed to be University), Haridwar, 249404, Uttarakhand, India
[b] Department of Environmental Science & Engineering, Indian Institute of Technology (Indian School of Mines), Dhanbad, 826004, India

ARTICLE INFO

Article history:
Received 21 August 2020
Received in revised form 25 January 2021
Accepted 16 April 2021

Keywords:
Scenedesmus sp. NC1
Fatty acid methyl ester (FAME)
Compensatory base pair changes (CBCs)
Autoflocculation
Biodiesel
Internal transcribed spacer 2 (ITS2)

ABSTRACT

An autoflocculating microalgal strain was isolated from coal mine effluent wastewater which was named as *Scenedesmus* sp. NC1 after morphological and molecularly characterization. Further analysis of internal transcribed spacer 2 (ITS2) and compensatory base changes (CBCs) showed it does not belong to the clade comprising *Scenedesmus sensu stricto*. In stationary phase of growth, *Scenedesmus* sp. NC1 exhibited excellent autoflocculation efficiency (> 88 %) within 150 min of setting. Temperature, pH, and inorganic metals exhibited minor influence on the autoflocculation activity of *Scenedesmus* sp. NC1. The fatty acid profiling of *Scenedesmus* sp.NC1 showed that palmitic acid (C16:0), oleic acid (C18:1), and stearic acid (18:0) accounted for more than 68 % of total fatty acids. Moreover, *Scenedesmus* sp. NC1 demonstrated significant bioflocculation potential over non-flocculating freshwater microalgae, *Chlorella* sp. NCQ and *Micractinium* sp. NCS2. Hence, *Scenedesmus* sp. NC1 could be effective for economical harvesting of other non-flocculating microalgae for productions of biodiesel and other metabolites.

1. Introduction

Microalgae are very diverse organisms; they belong to both the prokaryotic and the eukaryotic domains of the life tree. They are responsible for almost 50 % of organic carbon fixation globally [1]. Microalgae can efficiently convert solar energy into chemical potential energy than terrestrial plants. They are supposed as a better possible feedstock for bioenergy, such as biogas, biodiesel, and various other bioproducts, and they are very efficient in synthesizing and accumulating a high amount of lipids in the form of triacylglyceride (TAG) [2]. Microalgae help in the bioremediation of various types of wastewater by assimilating nutrients such as phosphorous and nitrogen present in wastewaters [3]. Apart from the bioenergy prospect microalgal biomass production is advantageous for mitigation of carbon dioxide (CO_2), because depending on the species microalgae have 10–50 times higher CO_2 sequestration activity than terrestrial plants [4].

Biomass-based biodiesel provides a hopeful alternative for principal energy sources, such as fossil fuel and nuclear-based energy, and is a good source for the mitigation of greenhouse gases. In the present time, the primary feedstock that is being utilized for commercial biodiesel production includes oil crops such as sunflower, soybean, jatropha, and animal fats, But biofuel production from these oil crops compromises the availability of various other valuable products such as food, fodder [5] Microalgae are a sustainable source for biodiesel energy; they belong to photosynthetic organisms that are very efficient in fixing inorganic carbon into various valuable products such as biofuels, pharmaceutical products, and many other biologically active compounds [6].

Isolation of a pure and axenic strain of microalgae from natural sources is significant for applying these microalgae in research, biochemical examination, and commercial application in various potential feedstock such as aquaculture, bioenergy, and bioprospecting. Microalgal culturing is a very daunting task as they are susceptible to physical and chemical parameters such as pH, temperature, and light intensity [6]. Conventional techniques applied for the isolation of microalgae cannot avoid the clumping/aggregation of cells, so that there is a possibility of the formation of the colony from more than one cell in place of a single cell [7]. Microscopic manipulation is a suitable method for isolating single intact cells without any damage and reduced contamination [8].

Microalgal dewatering is the most significant bottleneck in the production of microalgal products at the industrial scale. As dewatering of microalgae from its culture cost around (20 %–30 %) of total biomass production due to the small size (2−30 μm) as

* Corresponding author.
E-mail address: cbanerjee310@gmail.com (C. Banerjee).

https://doi.org/10.1016/j.btre.2021.e00621

well as lesser biomass concentrations (0.1–5.0 g/L) of microalgal cultures [9]. Generally, microalgae dewatering is achieved by adding substances known as flocculants, which could be natural or modified polymeric substances and inorganic chemicals [10]. Though the chemical flocculants are very useful in the dewatering of microalgae, those are generally not used for biomass dewatering when the desired end product is related to food, nutritional products, or high-value products [11]. Various techniques like centrifugation, flotation, sedimentation, filtration, flocculation, electrolytic, acoustic, and magnetic methods are currently used to harvest microalgal biomass. However, no particular method is delineated that is universally applicable to all microalgal species as every method has inherent disadvantages that affect the overall economics in downstream processing [12]. Therefore, the isolation and culturing of autoflocculating microalgal strain could be a valuable step towards the low-cost dewatering of microalgal biomass resources for the economic commercialization of biodiesel, food, supplements, as well as various other commercially relevant products derived from the microalgae.

The present paper describes the isolation of pure and axenic autoflocculating green microalgae through microscopic manipulation from the coal mine effluent environment. The isolated microalgal strain was taxonomically identified through molecular approaches, using compensatory base changes (CBC) in the internal transcribed spacer two (ITS2) region of the nuclear ribosomal RNA (rRNA) region. The identification of microalgal strains solely on the morphological features is unreliable due to interspecific similarity and intraspecific variations [12]. Besides, the morphological appearance of some microalgal strains differs with the age and culture conditions. Therefore, the ITS2 database, where the entire set of sequences and structure database acts as a template, facilitates the secondary structure prediction either through homology modeling or through direct folding [13]. Moreover, The ITS2 database also provides a BLAST search facility with specific ITS2 sequences, enabling the correct identification of newly isolated microalgal strains to their nearest relatives [14]. Additionally, the autoflocculation behavior of the isolated strain was studied towards the change in pH, temperature, time, and metal ion concentration. Moreover, the flocculation efficacy of isolated strain towards the non-flocculating microalgal freshwater microalgal strains *Chlorella* sp. NCQ and *Micractinium* sp. NCS2, respectively, was studied. The biomass composition in terms of protein, carbohydrate, and lipids was studied to provide a holistic approach towards the applicability of microalgal biomass as a sustainable and renewable energy source.

2. Materials and methods

2.1. Analysis of coal mine effluent wastewater

The biological oxygen demand (BOD_5), chemical oxygen demand (COD), total phosphate (TP), total nitrogen (TN), and Ammonical nitrogen (NH_3-N) of the water sample were estimated by following the standard methods, 5210 B, 5220 C, 4500 P.B.5 and 4500-N C, respectively (APHA, 2012). The pH and temperature of the water sample were estimated using the instrument, HANNA (HI2202). Different metals in the effluent mine water were estimated through atomic absorption spectrophotometer (AAS) (Perkin-Elmer AAnalyst ^{TM} 800, USA). Sodium (Na) and potassium (K) were estimated through flame photometer (Microprocessor based, Model 128).

2.2. Charge characteristics study of microalgae

The surface charge of microalgae affects the stability of microalgal culture, cultures with less magnitude of zeta potential values are less electrostatically stable than cultures with high magnitude of zeta value [12].The surface charge/ Zeta potential (ζ) of microalgae during different growth stages were determined through electrophoretic light scattering instrument zeta Sizer Nano ZS (Malvern, UK).

2.3. Sample collection, purification, and isolation

Microalgal samples were collected from coalmine effluent (Table 1) (23°82′N, 86°43′E) located in Dhanbad, India. In order to remove the contaminants and probable predators of microalgae like protozoa, rotifers, samples were quickly filtered by filtering sieve with the mesh size of 60 μm, 120 μm [15]. Microalgal samples obtained from the natural environment are usually contaminated with microbes. Therefore, the samples were first purified thrice by washing through centrifugation at 5000 rpm for 5 min. The biomass pellets were eventually resuspended in media containing a cocktail of filter (0.22 μm) sterilized antibiotic solutions containing 50 μg/mL nystatin, 200 μg/mL kanamycin, and 500 μg/mL cefotaxime [12]. It was essential to use different mixtures of the broad spectrum of antibiotics because bacteria might have different sensitivity for each antibiotic [16].

2.4. Isolation and purification of microalgae

Unicellular microalgal cells were isolated using microscopic manipulation techniques [7]. Briefly, the sample obtained after filtering and enrichment steps are complex mixtures of various microalgal strains. Samples were diluted tenfold by using autoclaved Tris-Acetate Phosphate (TAP) media comprised of [20 mM tris-base, 7 mM NH_4Cl, 0.45 mM $CaCl_2.2H_2O$, 0.83 mM $MgSO_4.7H_2O$, 1.05 mM KH_2PO_4, 1.65 mM K_2HPO_4, 1 mL/L of trace elements solution (134 μM Na_2EDTA. $2H_2O$, 184 μM H_3BO_3, 136 μM $ZnSO_4$. $7H_2O$, 40 μM $MnCl_2.4H_2O$, 32.9 μM $FeSO_4.7H_2O$, 12.3 μM $CoCl_2.6H_2O$, 10 μM $CuSO_4.5H_2O$, 4.44 μM $(NH_4)6MoO_3$) and 1 mL/L acetic acid]. An aliquot of dilute culture was taken on a sterile microscopic slide under the inverted microscope (Leica DMI6000) and subsequently smeared as a thin film. A small volume (0.2 μL) of sterile TAP media was put on the slide by micropipette; the algal cell got detached from the slide and became resuspended in the droplet. The obtained droplet containing suspended microalgal particles was transferred to another slide and again spread across the slide. The steps were repeated until a single targeted microalgal cell was obtained in the droplet. The single microalgal cell contained in the droplet transferred to the Petri dish, having solidified TAP media. After three days of incubation in the culture lab conditions, at temperature (25°C ± 2 °C), the light intensity of (100–120) μmol m^{-2} s^{-1} and with a photoperiod of 12:12 light-dark cycles, the pure green substantial single microalgal colony appeared [12,17]. After one week of incubation, the isolated

Table 1
Nutrient and physicochemical characterizations of coalmine effluent wastewater.

Parameters	Estimated values
pH	6.58 ± 0.88
Temperature (°C)	27.9 ± 0.97
BOD_5 (mg/L)	42 ± 2.6
COD (mg/L)	138 ± 3.7
TN (mg/L)	25.27 ± 3.1
TP (mg/L0	1.21 ± 0.03
NH_3-N (mg/L)	19.24 ± 0.9
Na (mg/L)	13.24 ± 0.08
K (mg/L)	9.27 ± 0.57
Fe (mg/L)	0.31
Mn (mg/L)	0.089
Zn (mg/L)	0.192
Ca (mg/L)	98.27 ± 3.84

microalgae did not show any sign of bacterial growth streaked onto another Petri plates containing solid algal growth media supplemented with antibiotic cefotaxime (500 μg/mL). The unialgal contamination-free colony of the isolated strain was inoculated through scrapping to a 5 mL capped glass tube containing 2 mL TAP media and incubated for 7 days under the specified conditions. After one week of incubation, the microalgal isolate was subcultured to a 100 mL flask containing 20 mL TAP media, and finally, it was scaled up to 2 L culture volume. The sample was examined microscopically and repeated plating and subculturing throughout the study to confirm a single strain.

2.5. Microalgal strains screening and determination of growth kinetic parameters

Microalgal cultivation was carried out in TAP media in 250 mL conical flasks with a working volume of 150 mL and cultivated under conditions described earlier. The microalgae growth was monitored by measuring the optical density at 680 nm using a spectrophotometer (Shimadzu, UV-1900 Japan). All the measurements were resultant of three triplicates. The microalgal specific growth rate (μ) was estimated by Eq. (1), doubling time (DT) by Eq. (2), and the microalgal biomass productivity (P) of the cultures was calculated by Eq. (3) [18].

$$\text{Specific growth rate } \mu\ (\text{d}-1) = \frac{(lnX_2 - lnX_1)}{(t_2 - t_1)} \quad (1)$$

Here, X_1 and X_2 are the dry weight biomass concentrations (g L^{-1}) of microalgae on days t_1 (start of the log phase) and t_2 (end of the log phase), respectively.

$$\text{Doubling time (DT)} = \ln(2) \times \mu^{-1} \quad (2)$$

$$\text{Biomass productivity (P) (g L} - 1\ \text{d} - 1) = \frac{X_2 - X_1}{t_2 - t_1} \quad (3)$$

Where $\boldsymbol{X_1}$ and $\boldsymbol{X_2}$ represent the dry weight biomass concentrations (g L^{-1}) of microalgae on days $\mathbf{t_1}$ initial day of culture, and $\mathbf{t_2}$ is the final day (in number) of culture, respectively.

2.6. Genomic DNA extraction, PCR amplification, and sequencing

For the microalgae's molecular identification, the genomic DNA was extracted through the modified CTAB extraction process [12]. Briefly, microalgal culture suspension was dewatered through centrifugation at 8000 rpm for 5 min. After proper washing, the biomass pellet was resuspended in 500 μL CTAB extraction buffer and incubated for 30 min at 65 ℃ for the lysis of microalgal biomass, followed by cooling at ambient temperature. Then, 500 μL of chilled chloroform and isoamyl alcohol (24:1) added and centrifuged at 13,000 rpm for 20 min. The aqueous phase was transferred to another tube, an equal volume of chilled isopropanol, and 50 mL of 3 M sodium acetate (pH 5.2) was added. Subsequently, the mixture was incubated at - 20 ℃ for one hour, then centrifuged at 13,200 rpm for10 min. Subsequently, the supernatant was gradually discarded, while the obtained genomic pellet was washed with cold 70 % ethanol and dried at ambient temperature. Eventually, the pellet was resuspended in 50 μL of (1 X) TE buffer. The obtained genomic fractions were visualized through electrophoresis on 0.8 % TAE agarose gel.

For amplification of genomic DNA, two sets of oligonucleotide PCR primers: Forward: 5`-GAAGTCGTAACAAGGTTTCC-3` and Reverse:5`-TCCTGGTTAGTTTCTTTTCC-3`.were used to amplify the complete internal transcribed spacer (ITS) ribosomal regions [12]. The PCR amplification of specific genomic segment was accomplished using 1x PCR buffer (5 mM KCl; 2 mM Tris−HCl pH 8.4), (60–100) ng/μl genomic DNA template, 1.5 mM $MgCl_2$, 0.2 mM dNTPs, 1 μM primer each and (5U/μl) Taq DNA polymerase. The thermal conditions for amplification comprises: initial incubation at 95 ℃ for 10 min followed by 30 amplification cycles at 95℃ denaturation for 30 s; primer amplification at 50℃ for 30 s and extension at 72 ℃ for 30 s followed by a final extension at 72℃ for 10 min [19]. The PCR amplicon was examined through electrophoretic separation on 1.2 % TAE agarose gel and purified using a gel extraction kit (Qiagen, Hilden, Germany).

The ITS sequences obtained were examined visually, and where required, it was edited manually in BioEdit (version 7.2.5) to eliminate non-overlapping sequences in 5' and 3' region. Moreover, the microalgal molecular identification was performed through the analysis sequence similarity using BLAST (Basic Local Alignment Search Tool) in the public database National Center for Biotechnology Information (NCBI). Moreover, the sequences were submitted to the NCBI gene bank under the accession number MG756652.1.

2.7. ITS2 secondary structure prediction, species delimitation through compensatory base changes (CBC), and phylogenetic analyses

The specific ITS2 region was identified and delimited from the complete ITS sequences obtained for the microalgae through the Hidden Markov model (HMM) based tool available in the ITS2 database [20]. Moreover, for analyzing the taxonomic positions of the new microalgal isolate, several ITS2 rRNA sequences of other homologous microalgal strains were retrieved through the BLAST search from the ITS2 database. The sequence and structure alignment was performed through the software program 4SALE v1.7.Which utilizes the 12 × 12 ITS2 specific matrix composed of three structural states (paired right, paired left, or unpaired) for every four nucleotides to align the primary sequence and structures synchronously [21]. Furthermore, The structure viewer and the CBC analyzer, as implemented in the program 4SALE v1.7, were employed to construct the ITS2 secondary structures and calculation of the CBC matrix [21]. Consensus structures were constructed by selecting multiple sequences, while a single sequence was selected to obtain the individual secondary structure.

The phylogenic history of the microalgal isolate was inferred by reconstruction of the phylogenic trees using maximum likelihood (ML) method [22]. The ITS2 sequences were aligned by ClustalW and finally the phylogenetic tree were obtained using program MEGA-X using default settings with Bootstrap support on 1000 pseudo-replicates [23].

2.8. Protein, carbohydrate, lipid, and pigment content of microalgae

The carbohydrate content in the microalgae was estimated spectrophotometrically through the phenol-sulphuric acid method [17]. Concisely, the dried microalgae were resuspended in 0.5 mL of deionized water afterward, 0.25 mL of 5% phenol solution was added, the obtained solution mixed with 1.25 mL of 98 % sulphuric acid. Subsequently, the mixture was retained at ambient temperature for 10 min. Finally, the absorbance of the resulting yellow-orange colored solution was recorded at wavelength 490 nm (Shimadzu, UV-1900 Japan). The carbohydrate content in biomasses was calculated using the standard curve using glucose as the standard [17].

The protein content was estimated by the colorimetric method with some modifications. 50 mg of lyophilized microalgal biomass mixed with 10 mL of deionized water and sonicated for 30 min. Subsequently, microalgal proteins were extracted by mixing an equal volume of biomass suspension with 2 N sodium hydroxide,

followed by heating at 90 ℃ for 10 min. After cooling sufficiently at room temperature, the extracted mixture was centrifuged at 4000 rpm for 5 min. The supernatant was collected, and residues were subjected to the same solvent extraction process. Finally, the supernatant was combined, and residues were discarded. The extracted protein samples were analyzed by measuring the absorbance (Shimadzu, UV-1900 Japan) at OD_{590} and OD_{460} and obtaining the OD_{590} /OD_{460} ratio [24]. The protein content was determined by constructing a standard curve using Bovine Serum Albumin (BSA) (dissolved in 0.15 M NaCl salt solution) protein as a standard.

The lipid content of microalgae was estimated spectrophotometrically through the sulpho-phospho-vanillin (SPV) method [25]. Briefly, two (2) ml of microalgal suspension was harvested through centrifugation at 8000 rpm for 5 min. The supernatant was discarded while the biomass was washed with deionized water and finally resuspended in 0.1 mL of deionized water. Then, 2 mL of concentrated sulphuric acid (H_2SO_4) was added to the suspension, and the mixture was incubated at 100 °C for 10 min. Eventually, after cooling the sample mixture, 5 mL of the freshly prepared sulpho-phospho-vanillin solution was added, and absorbance was recorded at 530 nm. The standard curve for the estimation of lipid content was prepared using triolein as standard lipid.

2.9. Lipid profiling through fatty acid methyl ester (FAME) analysis

Microalgal total lipids were extracted by following the method adopted from Bligh and Dyer [26] with some modifications. Concisely, 500 mg of lyophilized microalgal biomass was mixed with 15 mL of (2:1) chloroform: methanol (v: v) and incubated for 8 h at ambient temperature. The obtained mixture was filtered using 0.2 μm; GF/C filters (Whatman). The solid residues are subjected to the same extraction process. The combined filtrate was mixed with 25 mL of 5 % sodium chloride (w/v) solution in a separating funnel. The lipid-containing lower fraction collected in a round bottom flask and concentrated through the rotary evaporator. Finally, the extracted total lipid was measured gravimetrically. The extracted lipids were derivatized into FAMEs through acid-catalyzed transesterification, as described in [9]. FAMEs were analyzed using gas chromatography (Model GC 2010, Shimadzu, Kyoto, Japan) equipped with a flame ionization detector, and separation was accomplished by capillary column (Rtx-Wax, Restek). 1 μL sample volume was injected into the injection chamber at a temperature of 250 ℃. Helium gas with a flow rate at 0.40 mL/min was used as the carrier gas. Initial column temperature kept at 80℃ for 1 min, and subjected to increment by 40 ℃ min^{-1} to 160 ℃ for 2 min, the second ramp of 5 ℃ min^{-1} to 185 ℃ for 4 min, that was ramped at 30 ℃ min^{-1} to 280 ℃ for 2.5 min, and finally held for 3 min. The detector temperature was held at 230℃. The individual FAME peak was identified through their respective retention time by comparing it with the reference FAME standards (Supleco FAME -37 standards).

2.10. Auto flocculation study of microalgae

In order to estimate the autoflocculation efficiency, 200 mL of the microalgae were taken in the flask and gently mixed for 2 min through a magnetic stirrer. Samples were allowed to settle at room temperature for sufficient time, and no chemical was added until and unless stated. The auto flocculation behavior of microalgae was calculated owing to a change in the optical density (OD_{680}) of microalgal culture suspension using a UV–vis spectrophotometer (Shimadzu, UV-1900 Japan). After settling, the sample supernatants were pipetted out from 5 cm below the surface for evaluation of flocculation. The dewatering/flocculating efficiency was calculated, applying the formula described in Eq. (4) [12].

$$\text{Flocculation efficiency}: \ \eta\ (\%) = \frac{OD_{680(t0)} - OD_{680(t)}}{OD_{680(t0)}} \times 100 \quad (4)$$

Where $OD_{680(\mathbf{to})}$ is the optical density before flocculation (control), and $OD_{680(\mathbf{t})}$ is at a time (t), respectively.

For a better understanding of the autoflocculation properties of *Scenedesmus* sp. NC1, the effects of temperature, time, metal ions, and pH on the autoflocculation efficiency of microalgae was determined. The effect of time on the autoflocculation efficiency was studied by taking a 15 days old culture, and the flocculation efficiency was calculated at an interval of 30 min for 3.5 h. The effect of pH on the autoflocculation was studied by varying the pH of the culture at desired value ranging from 5 to 12 using either 1 M NaOH or 1 M HCl. The microalgal culture with unaltered pH was taken as control. To determine the effect of temperature on autoflocculation, the microalgae was incubated at temperature 15 °C–60 °C for and the microalgae at room temperature (28 °C) was used as control. Whereas, the metal salts $CaCl_2$, $MgCl_2$, $AlCl_3$, $FeCl_3$, and NaCl at concentration 10–30 mM used as a coagulant aid to study the effect of the inorganic chemicals on the dewatering of *Scenedesmus* sp. NC1. In blank preparation no any coagulant aid was added.

2.11. Bioflocculation of non-flocculating microalgae with Scenedesmus *sp. NC1*

The dewatering potential of autoflocculating microalgae *Scenedesmus* sp. NC1 towards non-flocculating microalgae was examined. Before the test, fifteen-day-old microalgae *Scenedesmus* sp. NC1 was harvested through centrifugation at 8000 rpm for 5 min. The cell-free supernatant was collected while the microalgal biomass pellets were washed with deionized water to remove media salts and finally resuspended in an equal volume of deionized water. The flocculation potential of the supernatant and the cell suspension was studied to harvest the previously isolated non-flocculating microalgal strains viz; *Chlorella* sp. NCQ and *Micractinium* sp. NCS2 in the stationary growth phase. The two non-flocculating microalgal strains were grown and cultured in TAP media under specified controlled conditions [12]. Dewatering experiments conducted using 20 mL of microalgal suspension in 50 mL polypropylene centrifuge tubes. The cell-free supernatant and the culture broth of the autoflocculating microalgal strain *Scenedesmus* sp. NC1, were added to non-flocculating microalgal suspension at ratio of 5%, 10 %, and 20 % (v/v) in triplicate. Afterward, the mixtures were agitated and allowed to settle at ambient temperature. Subsequently, the culture aliquot was taken at a depth of 3 cm, and absorbance was recorded at 680 nm using a spectrophotometer (Shimadzu, UV-1900 Japan). The flocculation efficiency was calculated using Eq. (4). The normal growing cultures of *Micractinium* sp. NCS2 and *Chlorella* sp. NCQ without *Scenedesmus* sp. NC1were used as control.

2.12. Statistical analyses

In this study, all the experiments were carried out in three independent biological replicates, and data were reported as mean ± standard error for each set of conditions. Statistical significance of the data was tested through one - way analysis of variance (ANOVA) using least significant difference with $p < 0.05$, and post-hoc analysis were conducted using Tukey's HSD test as implemented in software IBM SPSS 25.0.

3. Results and discussions

3.1. Isolation of microalgae

To execute any biotechnological or bioprospective activities, the selection and isolation of axenic, pure microalgae are necessary. Microalgae are adapted to exist in nearly all ecosystems available on the earth they are adapted for a wide range of environmental conditions. Microscopic studies show that the isolated microalgae are pure and have a colonial existence. In the present study, five microalgal strains *viz* NC-A, NC-B, NC-C, NC-D, and NC-E were isolated and studied under 40 X magnification through a Fluorescent microscope (Leica DM 3000, Germany). Among five isolated strains, only two (NC-A and NC-B) microalgal strains grew, and the rest turned brown during cultivation. NC-B was selected for further characterization and study, as it showed higher growth rates. Besides, the antimicrobial mixture, kanamycin 200 μg/mL, cefotaxime 500 μg/mL, and fluconazole 100 μg/mL was found to be very useful in the isolation of pure microalgal strains. Based on initial morphological appearances of isolate NC-B under 40 × magnification using a fluorescent microscope (Leica DM3000, Germany) and scanning electron microscopy (SEM) (JSM-6390LV, Jeol, Japan). The microalgal isolates belonged to the members of the division Chlorophyta. As microscopic and SEM image of the microalgal isolate revealed their colonial existence as the cells were forming distinct colonies consisting, coenobia of two-celled, and four celled, with protruding spines at the poles (supplementary Fig. 1). Although single elongated cells were also clearly visible. Therefore, the microalgae were identified as a member of the genus *Scenedesmus* [27].

3.2. Microalgal growth kinetic parameters

Biomass growth of microalgae *Scenedesmus* sp. NC1, in a batch cultivation mode, is represented in the Fig. 1. The results indicated a general increment in the microalgal biomass concentration of 1.02 g/L at day 13 and 0.97 g/L by day 16, where cultivation was terminated. There was a feeble increment in biomass up to day 3, representing the stationary growth phase. In contrast, the exponential phase of microalgal growth started from day 4 and happened for day 13, owing to an increase in biomass from 0.16 g/L to 1.02 g/L, respectively. After the late exponential phase, day 13, the microalgae enter into the stationary growth phase where the biomass was nearly constant, and on day 16, the biomass started to decline. The reduction in biomass growth could be attributed to the deficiency of nutrients in the growth media. Moreover, the microalgal *Scenedesmus* sp. NC1 exhibited a growth rate of 0.22 d^{-1} and biomass productivity of 0.096 g L^{-1} day^{-1}. Moreover, another essential parameter is represented in the Fig. 1 is the pH profile of microalgae during the cultivation period. The pH of the culture at the time of inoculation was (6.5 ± 0.06), the pH increased rapidly from the second day to the eighth day of cultivation (8.12 ± 0.012). After that, with a little variation, at the end of microalgal cultivation maximum pH of the microalgal culture was (8.78 ± 0.04). This increase in the pH of the microalgal culture during cultivation could be attributed to decrease in the CO_2 of the culture owing to increased photosynthetic activity of microalgae due to growth of biomass [28]

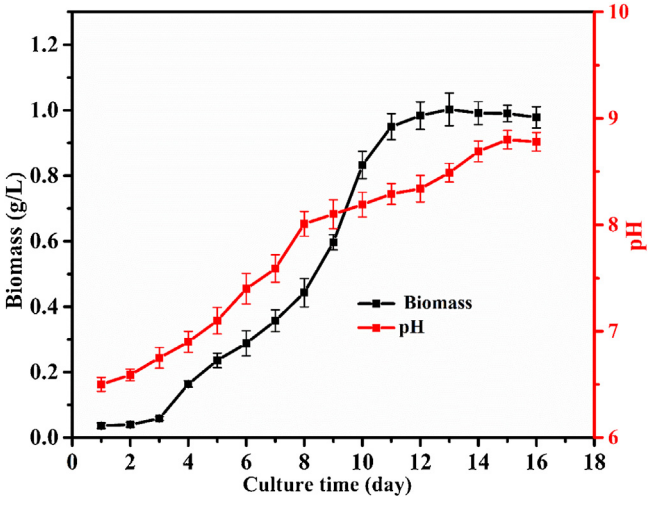

Fig. 1. Cell growth and pH profile of microalgae *Scenedesmus* sp. NC1, batch culture mode in TAP medium, over sixteen (16) days of incubation.

3.3. Genomic DNA extraction, PCR amplification, and sequencing

The universal forward and reverse primers were efficient and successfully amplified the desired segments of the genomic DNA. The sequence obtained from the amplified products of the nuclear ITS rDNA genomic region was around 0.652 kb in length. The BLAST analysis using ITS2 sequences revealed that microalgal isolate was closely related to microalgae belonging to genus *Scenedesmus* sp. DSA1 with 99 % identity (Table 2). Therefore, the microalgal isolate was identified as a member of genus *Scenedesmus* and named *Scenedesmus* sp. NC1.

3.4. ITS2 secondary structure prediction, species delimitation through compensatory base changes (CBC), and phylogenetic analyses

ITS2 consensus secondary structure was constructed using different accessions of the *Scenedesmus* genus. Fig. 2A, visualizes the complete sequence-structure alignment of the consensus structure (51 %) without any gap. The consensus structure revealed the typical core structure found in most of the eukaryotes comprising four helices (stems) which terminated in an apical loop. The helix III was the longest, with bulged regions and a single loop with UGG and GGU motifs near the apical region of the helix [29]. It was the most conserved helix with few variable bases present in the loop region. The helix II was folded into a hairpin loop with pyrimidine-pyrimidine (U-U) nucleotide mismatch. Helix II had more variable nucleotides than helix III distributed over the paired stem region. Besides, the A-rich region that differentiates the helix II and helix III was present in between the two helices [30]. The helix I had folded into a single hairpin loop with single bulged region near the basal portion of the stem. It had the highest variable nucleotides at the end of helix loop than helix II. While helix IV folded as the shortest helix among all the helices, which exhibited a single hairpin loop structure with a single internal bulged region at the basal portion of the helix.

Table 2
Molecular identification of indigenously isolated microalgae through sequence comparison of amplicon obtained through sequencing of ITS rDNA genomic region in NCBI database. Details of accession numbers, length of amplicon in base pairs, similarities between amplified sequences, and closest relative for sequences for freshwater isolated algae.

Microalgal strain Identified	Accession number	Length (nt)	Closest relative with accession number	Percent Similarity	Unidentified strain name
Scenedesmus sp. NC1	MG756652.1	652	*Scenedesmus* sp. DSA1 KX818838.1	99	NC-B

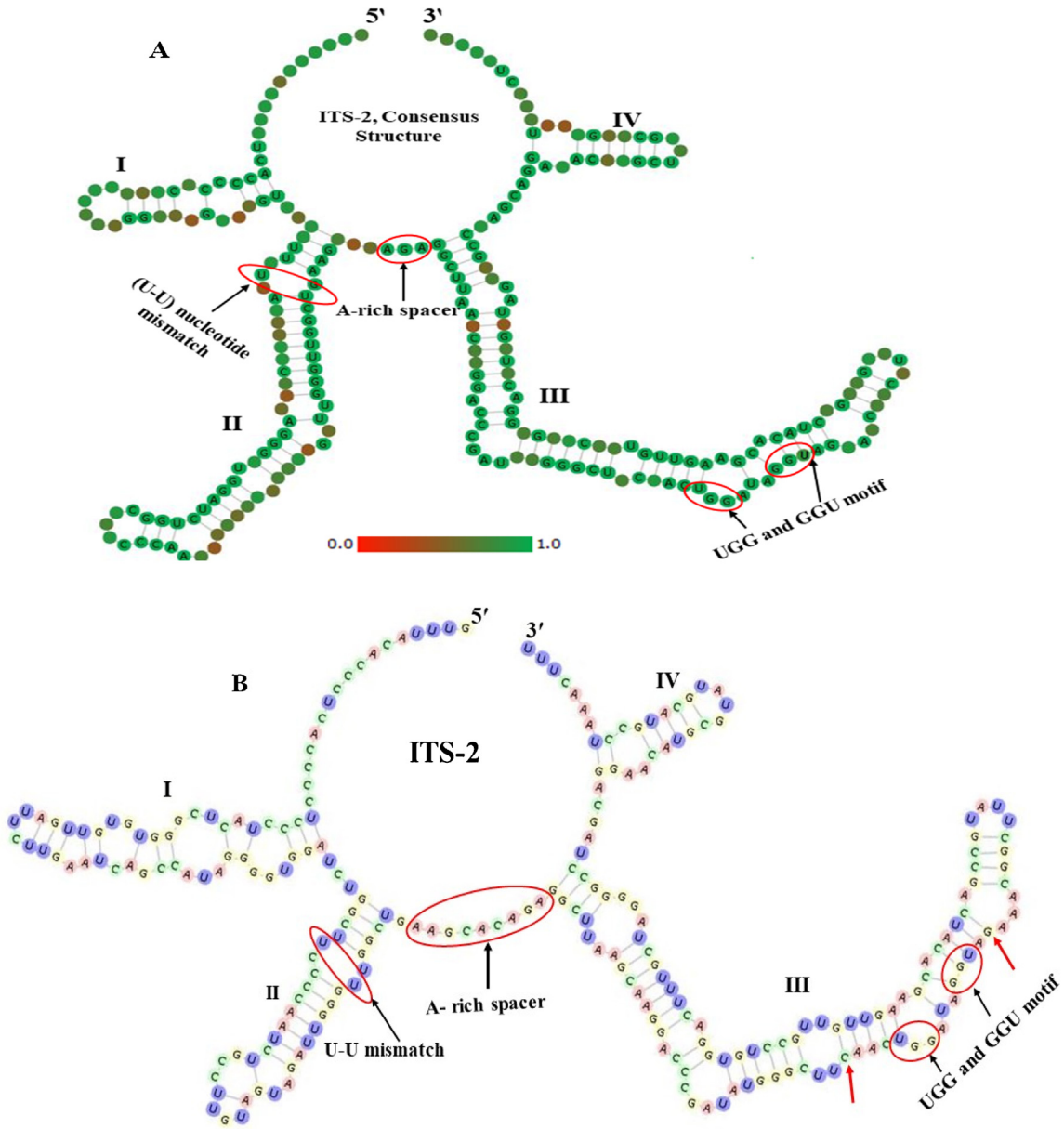

Fig. 2. (A) ITS-2 consensus secondary structure (51 %) without gap produced by 4SALE for: 1. *Scenedesmus* sp. NC1 MG756652.1, 2. *S. abundans* AJ400494.1, 3. *S. obtusus* AY170858, 3. *S. raciborskii* AJ237952, 4. *S. regularis* KF209348, 5. *S. acutus* AJ249508.1, 6. *S. hindakii* AY170856.1, 7. *S. bijugus* var. *obtusiusculus* KJ808697.1, 8. *S. armatus* JQ910904.1, 9. *S. regularis* KF209348. The four major helices are numbered I—IV, sequence conservation is represented from red brownish (not conserved) to green (conserved). Circles represents the different motifs. (B) ITS-2 secondary model without gap for microalgal isolate Scenedesmus sp. NC1 MG756652.1. Helices are numbered I—IV, characteristic ITS-2 motifs; A-rich spacer between helix I and III, U—U mismatch in helix II and universal conserved UGG and GGU motifs are demarcated by circles. Red arrow represents the position of 15 nucleotides conserved stretch. The figure was represented as visualized by 4 SALE.

ITS2 secondary structure of the *Scenedesmus* sp. NC1 is represented in Fig. 2B. The structure was folded into the typical secondary structure of eukaryotes with four helices interconnected through a spacer (unpaired nucleotide) [31]. Helix III was the largest which folded into different bulged motifs with at least one unpaired nucleotide region. The helix III had a stretch of 15 nucleotides (5′-CAACUGGAUAGGUAG-3′) long highly conserved region which confined the UGG and GGU motifs. Vanhannen et al. [32] had studied secondary structures of different *Scenedesmus* also reported the presence of such 15 nt long regions in helix III which were 100 % conserved. The helix II had the characteristic U—U bulge (mismatch) and the helix II was connected to helix III through conserved A- rich spacer [30]. Helix I was the second-largest helix that folded into a hairpin loop structure with prominent bulged regions. It showed unbranched conformation, which was characterized as general feature of the Sphaeropleaceae family that include green microalgae of genus *Scenedesmus* [31]. In contrast to other helices the helix IV emerged as the smallest among all. Moreover, the higher number of GC base pairing available at the paired regions retained the structural framework of the secondary structure.

The taxonomic studies concerning ITS2 genetic markers involve calculating compensatory base pair changes (CBC) for delimitation of species. CBC mentions the base - pair substitutions within the secondary structure, where nucleotide base pairs of a taxon are exchanged by different base pairs in another taxon [33]. The presence of even a single CBC in the conserved region of ITS2 is sufficient to delimit the species in sexual and asexual organisms

[34,35]. According to Muller et al. [34], the likelihood of two individuals belonging to different species within the same genus is 93.11 %; if there is at least one CBC is present in the ITS2 sequences. Conversely, if there is an absence of any CBCs, then there is a probability of 76.57 % that the individuals are members of the same species. Therefore, even there are no CBCs, they still probably be different species.

The calculation and recognition of CBCs from different ITS2 sequences were performed through 4SALE v1.7. In the comparable region of ITS2 secondary structure observed between Scenedesmus sp. NC1 and other accessions of genus *Scenedesmus* (Table 3) most of the CBCs were present in the highly conserved region of helix III. Helix IV had less CBCs than helix III while fewer CBCs were observed in helices I and II (Table 3). Three CBCs were observed between (MG756652.1) *Scenedesmus* sp. NC1 and (AY170856.1) *Scenedesmus. hindakii* which were detected in helix I, helix III, and IV. Furthermore, three CBCs each in helices I, II, and III were also observed between (MG756652.1) *Scenedesmus* sp. NC1and (KF209348) *Scenedesmus. regularis.* Whereas a total of 5 CBCs were observed between (MG756652.1) *Scenedesmus* sp. NC1and (AJ400494.1) *Scenedesmus. abundans* which were confined to the helix III only. The highest number of CBCs were present between *Scenedesmus* sp. NC1and (JQ910904.1) *Scenedesmus. armatus,* which were distributed in helix III and IV (Table 3). Only a single CBC was observed between *Scenedesmus* sp. NC1and (KF209348) *Scenedesmus. raciborskii* that was confined to helix IV.

Moreover, (KJ808697.1) *Scenedesmus bijugus* var. *obtusiusculus* and (JQ910904.1) *Scenedesmus armatus* do not showed any CBCs when compared with the isolate (MG756652.1) *Scenedesmus* sp. NC1, and both the accessions (KJ808697.1) and (JQ910904.1) clustered together with high bootstrap support (99) (Fig. 3). However, the isolate (MG756652.1) *Scenedesmus* sp. NC1 was more closely with (KX818838.1) *Scenedesmus* sp. DSA1 than (KF209348) *Scenedesmus. regularis* in an immensely supported clade. Hence it could be inferred that (MG756652.1) *Scenedesmus* sp. NC1 does not belong to *Scenedesmus* sensu stricto clade [*Scenedesmus. hindakii* (AY170856.1), and *Scenedesmus. obtusus* (AY170858)] (Fig. 3)

3.5. Protein, carbohydrate, lipid, and pigment content of microalgae

The biochemical composition of microalgal strain *Scenedesmus* sp. NC1 was estimated from the fifteen-day old culture at stationary growth phase. The isolate had substantial lipid content of 28.3 ± 1.2 %, with lipid productivity of 31.34 ± 1.9 mg L^{-1} d^{-1}. Whereas the total carbohydrate and protein content were 21 ± 1.05 % and 30 ± 1.5 % of total dry weight with corresponding productivities of 19.87 ± 0.48 mg L^{-1} d^{-1} and 26.2 ± 0.67 mg L^{-1} $d^{-1,}$ respectively. In a study *Scenedesmus. dimorphus* showed 26 % of lipid content in stationary growth phase when cultivated in BH-11 media with a light intensity of 42 μmol at temperature of 25 ± 2 °C [36]. A study performed by Shanmugam et al. [37] reported that *Scenedesmus*. sp cultivated in BG-11 media with a light intensity of 1500 lx, at temperature 25 °C having a photoperiod of 10 h light: 14 h dark exhibited 36 % lipid content. However, the thermotolerant strain *Desmodesmus* sp. F2 had 64.13 % lipid content with lipid productivity of 263 mg L^{-1} d^{-1}, while protein and carbohydrate content around 34.6 % and 31.5 %, respectively. When cultivated under high light intensity and temperature of 700 μmol/m^2s high and 35 °C respectively [39]. Hence, the mineral, nutrient composition, temperature, and light intensity used in the culture and cultivation significantly affect the metabolite composition of microalgae. These findings depicted that the isolated microalgae have considerable lipid content, to be efficiently applied as a feedstock for biodiesel production. In addition to that, the microalgal isolate exhibited an appreciable amount of protein and carbohydrate content; hence, it could be utilized as a feed supplement for aquatic organisms, animals and in the manufacturing of cosmetics and dietary supplements.

3.6. Lipid profiling through FAME analysis

One of the significant concerns of microalgal biomass harvesting is to use it as feedstock for the production of biodiesel. The lipid profile of *Scenedesmus* sp. NC1 is depicted in Table 4. The content of various fatty acids of microalgal lipid was ranging from C14-C20. The palmitic acid (C16:0) was the most abundant (24.54 ± 2.1 %) fatty acid, followed by oleic acid (C18:1) and linolenic acid (C18:3) with weight percent of 16.21 ± 1.1 % and 12.32 ± 1.3 %, respectively. While the other fatty acids, such as stearic acid (C18:0), linoleic acid (C18:2), palmitoleic acid (C16:1), and myristic acid (C14:0), were less than 12 % of total fatty acids. Simultaneously, arachidic acid (20:0) was the least abundant, accounting for 0.98 ± 0.58 % of total fatty acid. Various biofuel properties such as oxidative properties, cold flow properties, and cetane number solely depend on the chain length and degree of unsaturation of the biofuel constituents. Biodiesel with a higher amount of monounsaturated

Table 3
Frequency/Occurrence of two sided compensated base pair changes observed in the four helices between microalgal isolate Scenedesmus sp. NC1 and other related accessions from genus *Scenedesmus*.

	Scenedesmus. Sp. NC1				Number of CBCs
Taxon	Helix1	Helix2	Helix3	Helix4	
S. abundans AJ400494.1	0	0	139/222: A-U→G-C 141/220: U-G→A-U 152/213: U-A→A-U 179/190: A-U→G-C 180/188: C-G→G-C	0	5 CBCs
S. obtusus AY170858	0	0	139/222: U-A→G-C	242/255: G-C→A-U	2 CBCs
S.raciborskii AJ237952	0	0	0	242/255: G-C→A-U	1 CBCs
S. regularis KF209348	47/53: G-C→A-U	91/109: C-G→U-A	139/222: A-U→G-C	0	3 CBCs
S. hindakii AY170856.1	47/53: G-C→A-U	0	139/222: U-A→G-C	242/255: G-C→A-U	3 CBCs
S. armatus JQ910904.1	0	0	139/222: A-U→G-C 141/220: U-G→A-U 152/213: U-A→A-U 179/190: A-U→G-C 180/188: C-G→G-C	242/255: G-C→A-U 243/254: C-G→U-A	7CBCs
S. bijugus var. obtusiusculus KJ808697.1	0	0	0	0	NIL
S. acutus AJ249508.1	0	0	0	0	NIL
S sp. DSA1 KX818838.1	0	0	0	0	NIL

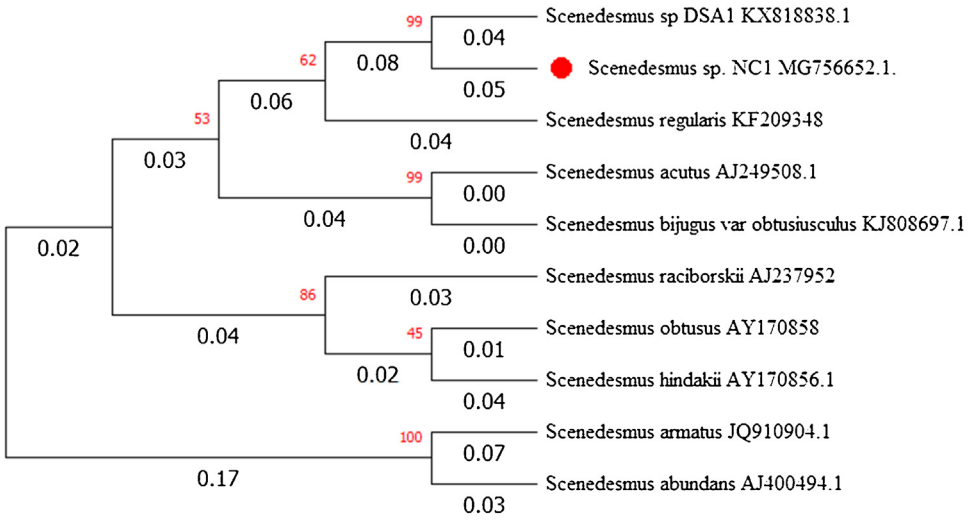

Fig. 3. A Maximum likelihood tree of the microalgal isolate *Scenedesmus* sp. NC1 and other microalgae from *Scenedesmus* genus based on ITS-2 Sequences. The numbers above the branches are the bootstrap values (≥50 %) for each branch and branch length are represented with precision of 2 places after decimal.

Table 4
Fatty acid composition of microalgal strain *Scenedesmus* sp.NC1 (wt %).

Fatty acids	Fatty acid composition (wt %)
Myristic acid (C14:0)	1.36 ± 1.7
Pentadecanoic acid (C15:0)	ND
Palmitic acid (C16:0)	24.54 ± 2.1
Palmitoleic acid (C16:1)	2.34 ± 0.21
Stearic acid (18:0)	8.27 ± 0.57
Oleic acid (C18:1)	16.21 ± 1.1
Linoleic acid (C18:2)	10.42 ± 1.5
Linolenic acid (C18:3)	12.32 ± 1.3
Arachidic acid (20:0)	0.98 ± 0.58
Others	23.56
Total saturated fatty acid (SFA)	35.15
Total mono unsaturated fatty acid (MUFA)	18.55
Total poly unsaturated acid (PUFA)	22.74
Ratio of unsaturated/saturated fatty acid	1.17

fatty acid (MUFA) and higher chain length have better oxidative stability, while polyunsaturated fatty acids (PUFA) content enhances the cold flow properties [40]. However, the content of monounsaturated (18.55 %), polyunsaturated (22.74 %), as well as saturated fatty acid (35.15 %) corroborates the compatibility towards biodiesel production as these fatty acids have better stability to fluidity and oxidation properties of biodiesel.

Moreover, the high content of oleic acid is the most favored quality of biodiesel as it provides a better balance between cold flow properties and stability of oxidation [41]. Moreover, several polyunsaturated fatty acids like linolenic acid linoleic acids are essential omega fatty acids, a vital dietary supplement for humans and animals. Hence, the present study reflects that the biomass of the microalgal strain *Scenedesmus* sp. NC1 has the potential to be used promising feedstock source for nutrients supplements and feedstock for biodiesel production.

3.7. Auto flocculation study of microalgae

The relationship between the autoflocculation behavior of the *Scenedesmus* sp. NC1 and the growth stages were studied, the autoflocculation behavior was monitored. As shown in Fig. 4, the autoflocculation behavior of the microalgae showed significant variation with the growth stages ($p < 0.05$). The settling activity increased parallel with microalgae growth stages, as shown in (Fig. 4), the autoflocculation efficiency increased drastically in the

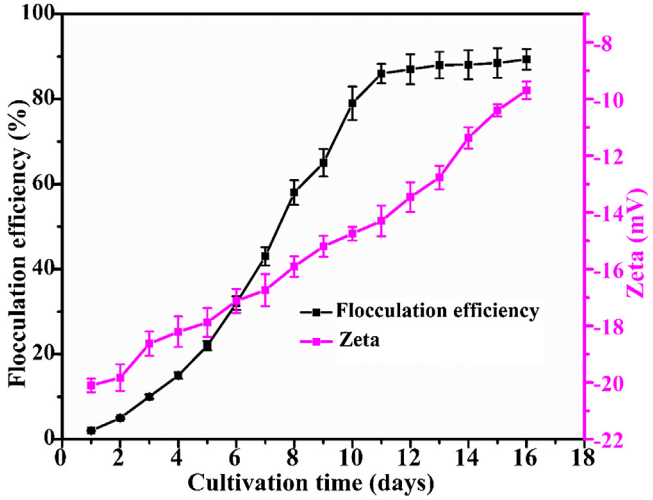

Fig. 4. Zeta potential and flocculation profiles of microalgal algal strain *Scenedesmus* sp.NC1 during batch culture condition.

exponential growth stage (> 75 %) than the lag phase (< 10 %). The biomass settling increased progressively during the exponential stage and (> 81 %) autoflocculation efficiency was observed at the end of exponential phase. Furthermore, the highest autoflocculation efficiency (89.31 ± 1.22) was observed in the stationary growth phase at fifteenth day of culturing. The autoflocculation activity of microalgae was more prominent in the late growth phase. The apparent surface charge/zeta potential (ζ) of microalgae of *Scenedesmus* sp. NC1 was monitored during growth stages (Fig. 4). The zeta potential decreased in magnitude during the growth stages from (-21.3 ± 1.2) at day 1 (lag-phase) to (– 14.64 ± 0.87) at day 10 (mid-exponential phase), to (-10.4 ± 1.26) at day 15, the stationary phase of growth. The decrease in the magnitude of zeta potential causes destabilization of the culture owing to reduction in the repulsive electrostatic forces among the microalgal cells [17]. The decrease in the magnitude of zeta potential at different growth stages was also observed in microalgae *Ettlia. Texensis* which had zeta-potential of -18.9 at the early exponential phase and remained -12.1 in stationary growth phase [42]. The results suggested that *Scenedesmus* sp. NC1 has auto/self-flocculation property that varied

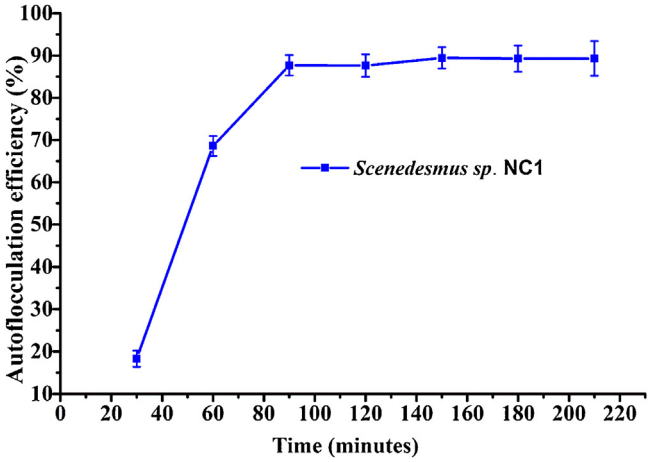

Fig. 5. The autoflocculation efficiency in fifteen day old microalgal isolate *Scenedesmus* sp. NC1 with respect to time at physiological pH.

with the growth stages. Hence, the effect of various factors on flocculation behavior was studied.

3.7.1. Effect of time on the autoflocculation

In the stationary phase the autoflocculation of *Scenedesmus* sp. NC1 was more impulsive. As in a 15 day old culture, within 90 min the microalgal settled at the bottom of the flask, leaving culture media with reduced microalgal concentration, as manifested by optical density 0.05−0.07. Hence, the effect of time variation on the autoflocculation efficiency was studied, and the results are represented in Fig. 5. The autoflocculation efficiency of the microalgae increased significantly ($p < 0.05$) with time. It showed the flocculation efficiency of 18.3 ± 1.24 % when the culture was allowed to settle for 30 min. As the duration of settling increased from 60−90 min, the flocculation efficiency increased from 68.57 ± 3.62 % to 88.32 ± 1.24 %, respectively. Moreover, the microalgae exhibited the highest autoflocculation efficiency of 89.46 ± 0.84 % at 150 min. Furthermore, no significant change in the flocculation efficiency was observed when settling time increased from150 min to 210 min, indicating the steady-state condition. Therefore, it was recommended that the microalgae *Scenedesmus* sp. NC1 was an efficient autoflocculating microalgae.

3.7.2. Effect of pH on the flocculation

The effect of culture pH on dewatering of *Scenedesmus* sp. NC1 was examined by changing the pH microalgal culture using either 1 M NaOH or 1 M HCl. When the culture pH reached at desired value ranged from 5 to 12, the autoflocculation efficiency was calculated. As shown in Fig. 6A, the culture pH showed a significant ($p < 0.05$) effect on autoflocculation of *Scenedesmus* sp. NC1. The dewatering of microalgae varied under different pH, at pH 8 and below significantly ($p < 0.05$) lesser autoflocculation efficiency was noted compared to control. As depicted in Fig. 6A, dewatering of *Scenedesmus* sp. NC1 was lower under acidulous conditions and showed 69.74 % efficiency at pH 5, which was significantly ($p < 0.05$) lower than control. At pH 9, no significant change ($p < 0.05$) in the dewatering of microalgae was noted as compared to positive control and resulted in 88.47 % flocculation efficiency. However, when the pH was further increased above 10, a significant increase in the flocculation was seen. The autoflocculation efficiency increased from 90.62–94.95 % when pH increased from 11 to 12. Several studies had reported that biomass dewatering was prominently affected by the microalgal culture pH. In microalgae *Ettlia* sp. YC00, the flocculation efficiency of > 60 % was noted at pH 10 which had increased to 86 % when pH was raised to 13 [43].

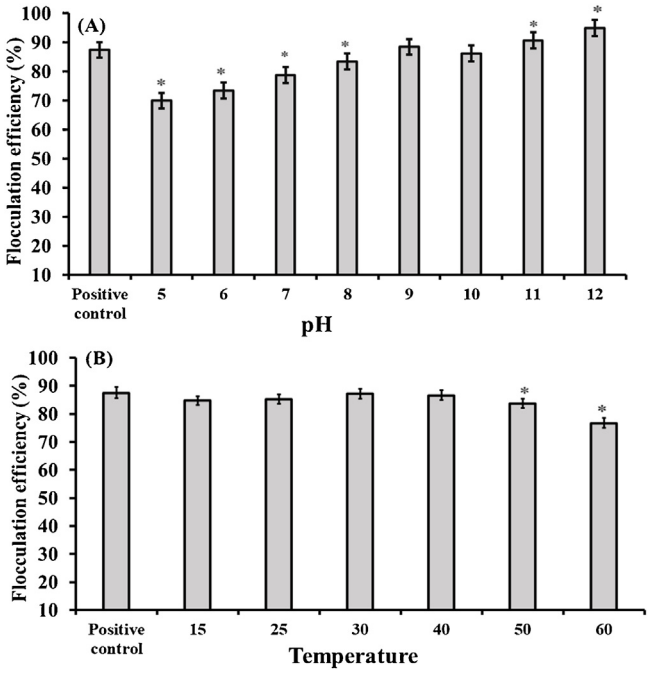

Fig. 6. The effect of different pH and temperature on the autoflocculation efficiency of Scenedesmus sp. NC1. All error bar denotes the standard error (SE) of three biological replicates. * indicates the statistical difference of $p < 0.05$ compared with the positive control.

Chen et al. [44] have also reported the increase in removal efficiency of self-flocculating microalge *Desmodesmus* sp. PW1 from 70 % to > 90 % when culture pH was increased from 3 to 12. The microalgae *Chlorella sorokiniana* 211−8 k, showed lowest removal effiency of 8.6 % at pH 9, whereas the highest flocculation efficiency of 97 % was noted at pH 13 [45]. The observed variation in the flocculation efficiency could have occurred due to change in the surface charge (Zeta potential) of the microalgal cell at changed pH conditions, which would have affected the flocculation capabilities of microalgal cells [44,28].Moreover, it has been reported that change in pH affects the dissolution of metal ions and the surface composition of microalgal cells are also affected [46].

3.7.3. Effect of temperature on flocculation

We studied the effect of temperature on the autoflocculation activity of *Scenedesmus* sp. NC1 by varying the temperature between 15 and 60 °C. As shown in Fig. 6B, the autoflocculation efficiency of microalgae exhibited significant difference ($p < 0.05$) under various culture temperatures. Under varied culture temperature, including 15, 25, 30, and 40 °C the *Scenedesmus* sp. NC1 showed the flocculation efficiency of 84.71, 85.25, 87.1, and 86.63 % respectively representing a minor change in autoflocculation efficiency than the positive control. However, the autoflocculation efficiency significantly ($p < 0.05$) decreased at higher temperature. As the flocculation efficiency decreased from 86.63 % to 76.72 %, when the culture temperature increased from 40 to 60 °C. Based on this study, the suitable temperature for biomass harvesting of *Scenedesmus* sp. NC1 at room temperature could be cost effective owing to higher autoflocculation efficiency of more than 87 %.

3.7.4. Effects of metal ions on the autoflocculation

Several studies had shown that various metal ions like aluminum (Al^{3+}), iron (Fe^{3+}), magnesium (Mg^{2+}) could improve microalgal harvesting when added into the microalgal culture suspension [47]. Cationic metal ions affect the stability and influence the flocculation of microalge generally by two

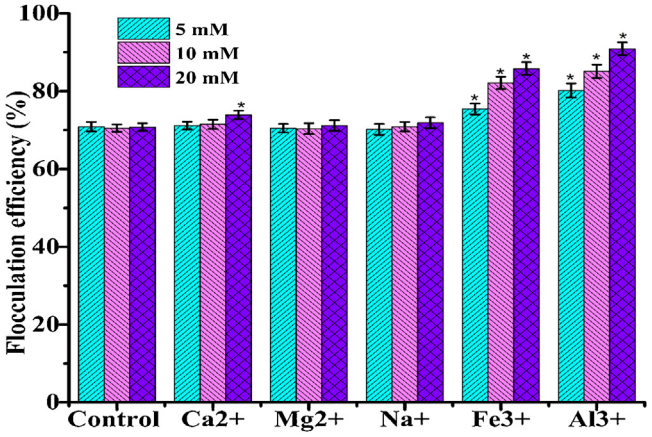

Fig. 7. The influence of different metals ions on the flocculation efficiency of *Scenedesmus sp*. NC1. Error bar denotes the standard error (SE) of three biological replicates. * indicates the statistical difference of $p < 0.05$ compared with the positive control.

mechanisms. Firstly, cationic metals interact directly with negatively charged cells and neutralize the microalgae [17]. Secondly, metals hydrolyses to metal hydroxides or interact with phosphate to produce positively charged ligand, which flocculate the microalgae through bridging or electric patch mechanisms (Rashid et al.,. 2019; Papazi et al., 2009). We investigated the influence of some metal ions on the autoflocculation activity of microalgae, *Scenedesmus* sp. NC1, the results are displayed in Fig. 7. No significant ($p < 0.05$) change in the flocculation efficiency of microalgal cells was observed when Ca^{2+}, Mg^{2+}, and Na^{+} were added to the culture suspension at 5 and 10 mM concentration. Calcium (Ca^{2+}) showed minor but significant ($p < 0.05$) change in flocculation efficiency at 20 mM concentrations, while Mg^{2+}, and Na^{+} remained insignificant at that 20 mM concentrations. However, Fe^{3+} and Al^{3+} exhibited a significant ($p < 0.05$) effect on flocculation at every concentration used in this study. More than 10 % increase in flocculation efficiency was observed at 20 mM of $Fe^{3+,}$ and more than a 20 % increase in flocculation than control was exhibited when 20 mM of Al^{3+} metal salts were provided to microalgal culture. Chen et al. [48] also reported that the metal ions Na^{+}, $K^{+,}$ and Mg^{2+} have no significant effect on the flocculation of microalgal strain *Desmodesmus* sp. PW1. Guo et al. [49] observed an increase in flocculation efficiency in microalgal strain Scenedesmus obliquus AS-6−1 when Al^{3+} was provided to the microalgal culture. Findings of different studies have shown that the flocculation of microalgae by the metal ion is dependent on the type of metal ion and the concerned microalgal species [50,51].

3.8. Bioflocculation of non-flocculating microalgae with Scenedesmus *sp. NC1*

Studies have reported that autoflocculating microalgae like, *Scenedesmus obliquus* AS-6−1, *Scenedesmus* rubescens SX, *Ankistrodesmus falcatus, Tetraselmis suecica,* have considerable potential to flocculate the non-flocculating microalgae and therefore could be employed as bioflocculant [52,53,49]. The bioflocculation potential of microalgal strain *Scenedesmus* sp. NC1 towards the non-flocculating microalgae *Chlorella* sp. NCQ and *Micractinium* sp. NCS2 using cell-free supernatant and culture broth was tested. The results are presented in the Fig. 8. The culture broth exhibited significant ($p < 0.05$) flocculation potential towards the non-flocculating microalgae *Chlorella* sp. NCQ and *Micractinium* sp. NCS2. In *Chlorella* sp. NCQ (Fig. 8A) the culture broth of *Scenedesmus* sp. NC1 exhibited the flocculation efficiency of 12.98 ± 2.08 % at ratio of 5 % (v/v). However, when the cell ratio

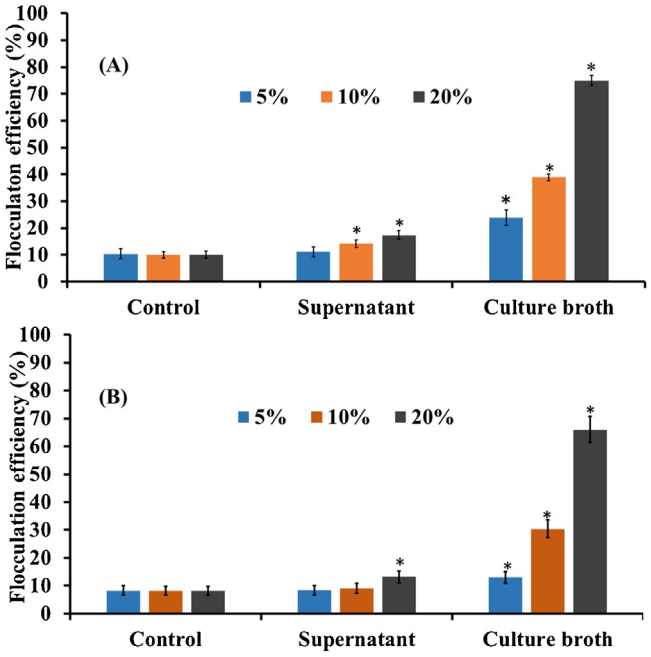

Fig. 8. Flocculation of non-flocculating microalgae *Chlorella* sp.NCQ and *Micractinium* sp. NCS2 with auto-flocculating microalgae *Scenedesmus* sp. NC1when the supernatant and the cell suspensions of the autoflocculating microalgal strain *Scenedesmus* sp.NC1, were added to non-flocculating microalgal suspension at ratio of 5% to 20 % (v/v). Error bar denotes the standard error (SE) of three biological replicates. * indicates the statistical difference of $p < 0.05$ compared to control.

was increased from 10 to 20 % (v/v) the flocculation efficiency increased from 30.27 ± 3.14 % to 66.17 ± 4.57 % respectively. As compared to *Chlorella* sp. NCQ the culture broth of *Scenedesmus* sp. NC1showed higher flocculation efficiency for microalgae *Micractinium* sp. NCS2 (Fig. 8B) at all tested cell ratios. As it showed 23.73 ± 2.13 % flocculation efficiency at ratio of 5 % (v/v). When the final ratio increased from 10 to 20 % (v/v) the flocculation efficiency increased from 38.09 ± 0.97 % to highest value of 73.98 ± 0.87 % respectively. Despite the culture broth the cell-free supernatant of the isolate had little flocculation activity owing to the flocculation efficiency of 13.17 ± 0.24 % and 17.36 ± 0.74 % at the final ratio of 20 % (v/v) for microalgae *Chlorella* sp. NCQ and *Micractinium* sp. NCS2 respectively. The observed variation in the flocculation efficiency could be due to the difference the surface charge of the microalgae *Chlorella* sp. NCQ (−24 mV) and *Micractinium* sp. NCS2 (−19.2 mV).

4. Conclusions

In this work, an autoflocculating microalgae was isolated from coal mine effluent wastewater named as *Scenedesmus* sp. NC1 after the morphological, molecular, and taxonomical examination. The CBCs evaluation in the conserved regions of the secondary structure of ITS2 revealed that the isolate *Scenedesmus* sp. NC1 does not belong to the clade comprising *Scenedesmus sensu stricto.* Moreover, the mixture of antimicrobial agents' fluconazole, cefotaxime, and kanamycin, was also proven effective for the isolation and maintenance of axenic microalgae. The biochemical composition of *Scenedesmus* sp. NC1 exhibited its potential to be used as a source of nutrients and biofuel production. The lipid characterisation examination demonstrated, different fatty acid compositions with monounsaturated (18.55 %), polyunsaturated (22.74 %), as well as saturated fatty acid (35.15 %). Indicating a promising candidate for biodiesel production. Furthermore, the *Scenedesmus* sp. NC1 exhibited admirable autoflocculating behavior which was dependent on the growth stages. Meanwhile, the

autoflocculation was slightly influenced by the variation of pH, temperature and inorganic metals. Moreover, the isolate exhibited, substantial bioflocculation efficacy towards freshwater microalgae *Micractinium* sp. NCS2 and *Chlorella* sp. NCQ with harvesting efficiency of 74 % and 66 %, respectively. Inclusively, *Scenedesmus* sp. NC1 was a bioflocculant with potential for biofuel production.

Declaration of Competing Interest

The authors report no declarations of interest.

Acknowledgments

Niwas Kumar sincerely acknowledges the Indian Council of Medical Research (ICMR), Government of India, New Delhi, for granting doctoral fellowship in the form of ICMR-JRF (3/1/3/JRF-2015/HRD) at IIT(ISM), Dhanbad. Chiranjib Banerjee sincerely acknowledges the financial support provided by the Department of Science and Technology (DST) Government of India, in the form of the INSPIRE faculty award scheme (DST/ INSPIRE Faculty Award /2014/ LSPA-25). The authors also acknowledge the DST-FIST program or providing infrastructure support.

Appendix A. Supplementary data

Supplementary material related to this article can be found, in the online version, at doi:https://doi.org/10.1016/j.btre.2021.e00621.

References

[1] R. León-Bañares, D. González-Ballester, A. Galván, E. Fernández, Transgenic microalgae as green cell-factories, Trends Biotechnol. 22 (2004) 45–52, doi:http://dx.doi.org/10.1016/j.tibtech.2003.11.003.
[2] B. Sajjadi, W.Y. Chen, A.A.A. Raman, S. Ibrahim, Microalgae lipid and biomass for biofuel production: a comprehensive review on lipid enhancement strategies and their effects on fatty acid composition, Renew. Sustain. Energy Rev. 97 (2018) 200–232, doi:http://dx.doi.org/10.1016/j.rser.2018.07.050.
[3] B. Porto, A.L. Gonçalves, A.F. Esteves, S.M.A.G.U. de Souza, A.A.U. de Souza, V.J.P. Vilar, J.C.M. Pires, Assessing the potential of microalgae for nutrients removal from a landfill leachate using an innovative tubular photobioreactor, Chem. Eng. J. (2020), doi:http://dx.doi.org/10.1016/j.cej.2020.127546.
[4] J. Cheng, Y. Zhu, Z. Zhang, W. Yang, Modification and improvement of microalgae strains for strengthening CO2 fixation from coal-fired flue gas in power plants, Bioresour. Technol. 291 (2019), doi:http://dx.doi.org/10.1016/j.biortech.2019.121850.
[5] Y. Chisti, Biodiesel from microalgae, Biotechnol. Adv. 25 (2007) 294–306, doi:http://dx.doi.org/10.1016/j.biotechadv.2007.02.001.
[6] T. Mutanda, D. Naidoo, J.K. Bwapwa, A. Anandraj, Biotechnological applications of microalgal oleaginous compounds: current trends on microalgal bioprocessing of products, Front. Energy Res. 8 (2020) 1–21, doi:http://dx.doi.org/10.3389/fenrg.2020.598803.
[7] J. Fröhlich, H. König, New techniques for isolation of single prokaryotic cells, FEMS Microbiol. Rev. 24 (2000) 567–572, doi:http://dx.doi.org/10.1016/S0168-6445(00)00045-0.
[8] T. Mutanda, D. Ramesh, S. Karthikeyan, S. Kumari, A. Anandraj, F. Bux, Bioprospecting for hyper-lipid producing microalgal strains for sustainable biofuel production, Bioresour. Technol. 102 (2011) 57–70, doi:http://dx.doi.org/10.1016/j.biortech.2010.06.077.
[9] S. Wang, M. Yerkebulan, A.E.F. Abomohra, S. El-Khodary, Q. Wang, Microalgae harvest influences the energy recovery: a case study on chemical flocculation of Scenedesmus obliquus for biodiesel and crude bio-oil production, Bioresour. Technol. 286 (2019) 121371, doi:http://dx.doi.org/10.1016/j.biortech.2019.121371.
[10] C. Banerjee, S. Ghosh, G. Sen, S. Mishra, P. Shukla, R. Bandopadhyay, Study of algal biomass harvesting using cationic guar gum from the natural plant source as flocculant, Carbohydr. Polym. 92 (2013) 675–681, doi:http://dx.doi.org/10.1016/j.carbpol.2012.09.022.
[11] N. Fuad, R. Omar, S. Kamarudin, R. Harun, A. Idris, W.A.K.G. Wan Azlina, Effective use of tannin based natural biopolymer, AFlok-BP1 to harvest marine microalgae Nannochloropsis sp, J. Environ. Chem. Eng. 6 (2018) 4318–4328, doi:http://dx.doi.org/10.1016/j.jece.2018.06.041.
[12] N. Kumar, C. Banerjee, N. Kumar, S. Jagadevan, A novel non-starch based cationic polymer as flocculant for harvesting microalgae, Bioresour. Technol. 271 (2019) 383–390, doi:http://dx.doi.org/10.1016/j.biortech.2018.09.073.
[13] C. Selig, M. Wolf, T. Müller, T. Dandekar, J. Schultz, The ITS2 Database II: homology modelling RNA structure for molecular systematics, Nucleic Acids Res. 36 (2008) 377–380, doi:http://dx.doi.org/10.1093/nar/gkm827.
[14] M.J. Ankenbrand, A. Keller, M. Wolf, J. Schultz, F. Förster, ITS2 database V: twice as much, Mol. Biol. Evol. 32 (2015) 3030–3032, doi:http://dx.doi.org/10.1093/molbev/msv174.
[15] M. He, L. Li, J. Liu, Isolation of wild microalgae from natural water bodies for high hydrogen producing strains, Int. J. Hydrogen Energy 37 (2012) 4046–4056, doi:http://dx.doi.org/10.1016/j.ijhydene.2011.11.089.
[16] M.R. Droop, A procedure for routine purification of algal cultures with antibiotics, Br. Phycol. Bull. 3 (1967) 295–297, doi:http://dx.doi.org/10.1080/00071616700650171.
[17] N. Kumar, C. Banerjee, S. Jagadevan, Cationically functionalized dextrin polymer as an efficient flocculant for harvesting microalgae, Energy Rep. 6 (2020) 2803–2815, doi:http://dx.doi.org/10.1016/j.egyr.2020.09.040.
[18] A.V. Piligaev, K.N. Sorokina, A.V. Bryanskaya, S.E. Peltek, N.A. Kolchanov, V.N. Parmon, Isolation of prospective microalgal strains with high saturated fatty acid content for biofuel production, ALGAL. 12 (2015) 368–376, doi:http://dx.doi.org/10.1016/j.algal.2015.08.026.
[19] M. Timmins, S.R. Thomas-Hall, A. Darling, E. Zhang, B. Hankamer, U.C. Marx, P. M. Schenk, Phylogenetic and molecular analysis of hydrogen-producing green algae, J. Exp. Bot. 60 (2009) 1691–1702, doi:http://dx.doi.org/10.1093/jxb/erp052.
[20] A. Keller, F. Förster, T. Müller, T. Dandekar, J. Schultz, M. Wolf, Including RNA secondary structures improves accuracy and robustness in reconstruction of phylogenetic trees, Biol. Direct 5 (2010) 1–12, doi:http://dx.doi.org/10.1186/1745-6150-5-4.
[21] P.N. Seibel, T. Müller, T. Dandekar, M. Wolf, Synchronous visual analysis and editing of RNA sequence and secondary structure alignments using 4SALE, BMC Res. Notes 1 (2008) 1–7, doi:http://dx.doi.org/10.1186/1756-0500-1-91.
[22] M.A. Buchheim, E.A. Michalopulos, J.A. Buchheim, Phylogeny of the chlorophyceae with special reference to the Sphaeropleales: a study of 18s and 26s rDNA data, J. Phycol. 37 (2001) 819–835, doi:http://dx.doi.org/10.1046/j.1529-8817.2001.00162.x.
[23] S. Kumar, G. Stecher, M. Li, C. Knyaz, K. Tamura, M.E.G.A. X, Molecular evolutionary genetics analysis across computing platforms, Mol. Biol. Evol. 35 (2018) 1547–1549, doi:http://dx.doi.org/10.1093/molbev/msy096.
[24] T. Zor, Z. Selinger, Linearization of the bradford protein assay increases its sensitivity, Anal. Biochem. 308 (1996) 302–308.
[25] A.R. Byreddy, A. Gupta, C.J. Barrow, M. Puri, A quick colorimetric method for total lipid quantification in microalgae, J. Microbiol, Methods. 125 (2016) 28–32, doi:http://dx.doi.org/10.1016/j.mimet.2016.04.002.
[26] E.G. Bligh, W.J. Dyer, Can. J. Biochem. Physiol. 37 (1959).
[27] K. Sciuto, L.A. Lewis, E. Verleyen, I. Moro, N. La Rocca, Chodatodesmus australis sp. nov. (Scenedesmaceae, Chlorophyta) from Antarctica, with the emended description of the genus Chodatodesmus, and circumscription of Flechtneria rotunda gen. et sp. nov, J. Phycol. 51 (2015) 1172–1188, doi:http://dx.doi.org/10.1111/jpy.12355.
[28] X. Lei, W. Zheng, H. Ding, X. Zhu, Q. Chen, H. Xu, T. Zheng, Y. Tian, Effective harvesting of the marine microalga Thalassiosira pseudonana by Marinobacter sp. FL06, Bioresour. Technol. 269 (2018) 127–133, doi:http://dx.doi.org/10.1016/j.biortech.2018.08.077.
[29] A. Toledo-Cervantes, G. Garduño Solórzano, J.E. Campos, M. Martínez-García, M. Morales, Characterization of Scenedesmus obtusiusculus AT-UAM for high-energy molecules accumulation: deeper insight into biotechnological potential of strains of the same species, Biotechnol. Rep. Amst. (Amst) 17 (2018) 16–23, doi:http://dx.doi.org/10.1016/j.btre.2017.11.009.
[30] J.S. Heeg, M. Wolf, ITS2 and 18S rDNA sequence-structure phylogeny of Chlorella and allies (Chlorophyta, Trebouxiophyceae, Chlorellaceae), Plant Gene 4 (2015) 20–28, doi:http://dx.doi.org/10.1016/j.plgene.2015.08.001.
[31] L. Caisová, B. Marin, M. Melkonian, A consensus secondary structure of ITS2 in the Chlorophyta Identified by phylogenetic reconstruction, Protist. 164 (2013) 482–496, doi:http://dx.doi.org/10.1016/j.protis.2013.04.005.
[32] E.J. Van Hannen, P. Fink, M. Lürling, A revised secondary structure model for the internal transcribed spacer 2 of the green algae Scenedesmus and Desmodesmus and its implication for the phylogeny of these algae, Eur. J. Phycol. 37 (2002) 203–208, doi:http://dx.doi.org/10.1017/S096702620200361X.
[33] R.R. Gutell, N. Larsen, C.R. Woese, Lessons from an evolving rRNA: 16S and 23S rRNA structures from a comparative perspective, Microbiol. Rev. 58 (1994) 10–26, doi:http://dx.doi.org/10.1128/mmbr.58.1.10-26.1994.
[34] T. Müller, N. Philippi, T. Dandekar, J. Schultz, M. Wolf, Distinguishing species, Rna. 13 (2007) 1469–1472, doi:http://dx.doi.org/10.1261/rna.617107.
[35] A.W. Coleman, Is there a molecular key to the level of "biological species" in eukaryotes? A DNA guide, Mol. Phylogenet. Evol. 50 (2009) 197–203, doi:http://dx.doi.org/10.1016/j.ympev.2008.10.008.
[36] T. Sharma, R.S. Gour, A. Kant, R.S. Chauhan, Lipid content in Scenedesmus species correlates with multiple genes of fatty acid and triacylglycerol biosynthetic pathways, Algal Res. 12 (2015) 341–349, doi:http://dx.doi.org/10.1016/j.algal.2015.09.006.
[37] S. Shanmugam, T. Mathimani, S. Anto, M.P. Sudhakar, S.S. Kumar, A. Pugazhendhi, Cell density, Lipidomic profile, and fatty acid characterization as selection criteria in bioprospecting of microalgae and cyanobacterium for biodiesel production, Bioresour. Technol. 304 (2020) 123061, doi:http://dx.doi.org/10.1016/j.biortech.2020.123061.

[39] S.H. Ho, J.S. Chang, Y.Y. Lai, C.N.N. Chen, Achieving high lipid productivity of a thermotolerant microalga Desmodesmus sp. F2 by optimizing environmental factors and nutrient conditions, Bioresour. Technol. 156 (2014) 108–116, doi: http://dx.doi.org/10.1016/j.biortech.2014.01.017.
[40] A.V. Piligaev, K.N. Sorokina, A.V. Bryanskaya, S.E. Peltek, N.A. Kolchanov, V.N. Parmon, Isolation of prospective microalgal strains with high saturated fatty acid content for biofuel production, Algal Res. 12 (2015) 368–376, doi:http://dx.doi.org/10.1016/j.algal.2015.08.026.
[41] G. Knothe, "Designer" biodiesel: optimizing fatty ester composition to improve fuel properties, Energy Fuels 22 (2008) 1358–1364, doi:http://dx.doi.org/10.1021/ef700639e.
[42] S. Salim, Z. Shi, M.H. Vermuë, R.H. Wijffels, Effect of growth phase on harvesting characteristics, autoflocculation and lipid content of Ettlia texensis for microalgal biodiesel production, Bioresour. Technol. 138 (2013) 214–221, doi:http://dx.doi.org/10.1016/j.biortech.2013.03.173.
[43] N. Rashid, M. Nayak, W.I. Suh, B. Lee, Y.K. Chang, Efficient microalgae removal from aqueous medium through auto-flocculation: investigating growth-dependent role of organic matter, Environ. Sci. Pollut. Res. 26 (2019) 27396–27406, doi:http://dx.doi.org/10.1007/s11356-019-05904-6.
[44] Z. Chen, S. Shao, Y. He, Q. Luo, M. Zheng, M. Zheng, B. Chen, M. Wang, Nutrients removal from piggery wastewater coupled to lipid production by a newly isolated self-flocculating microalga Desmodesmus sp. PW1, Bioresour. Technol. 302 (2020) 122806, doi:http://dx.doi.org/10.1016/j.biortech.2020.122806.
[45] L. de Souza Leite, L.A. Daniel, Optimization of microalgae harvesting by sedimentation induced by high pH, Water Sci. Technol. 82 (2020) 1227–1236, doi:http://dx.doi.org/10.2166/wst.2020.106.
[46] H. Yuan, X. Zhang, Z. Jiang, X. Wang, X. Chen, L. Cao, X. Zhang, Analyzing the effect of pH on microalgae adhesion by identifying the dominant interaction between cell and surface, Colloids Surf. B Biointerfaces 177 (2019) 479–486, doi:http://dx.doi.org/10.1016/j.colsurfb.2019.02.023.
[47] G.P. Sheng, H.Q. Yu, X.Y. Li, Extracellular polymeric substances (EPS) of microbial aggregates in biological wastewater treatment systems: a review, Biotechnol. Adv. 28 (2010) 882–894, doi:http://dx.doi.org/10.1016/j.biotechadv.2010.08.001.
[48] Z. Chen, S. Shao, Y. He, Q. Luo, M. Zheng, M. Zheng, B. Chen, M. Wang, Nutrients removal from piggery wastewater coupled to lipid production by a newly isolated self-flocculating microalga Desmodesmus sp. PW1, Bioresour. Technol. 302 (2020) 122806, doi:http://dx.doi.org/10.1016/j.biortech.2020.122806.
[49] S.L. Guo, X.Q. Zhao, C. Wan, Z.Y. Huang, Y.L. Yang, M. Asraful Alam, S.H. Ho, F.W. Bai, J.S. Chang, Characterization of flocculating agent from the self-flocculating microalga Scenedesmus obliquus AS-6-1 for efficient biomass harvest, Bioresour. Technol. 145 (2013) 285–289, doi:http://dx.doi.org/10.1016/j.biortech.2013.01.120.
[50] C. Wan, X.Q. Zhao, S.L. Guo, M. Asraful Alam, F.W. Bai, Bioflocculant production from Solibacillus silvestris W01 and its application in cost-effective harvest of marine microalga Nannochloropsis oceanica by flocculation, Bioresour. Technol. 135 (2013) 207–212, doi:http://dx.doi.org/10.1016/j.biortech.2012.10.004.
[51] T. Chatsungnoen, Y. Chisti, Flocculation and Electroflocculation for Algal Biomass Recovery, second edi, Elsevier B.V., 2019, doi:http://dx.doi.org/10.1016/b978-0-444-64192-2.00011-1.
[52] S. Salim, R. Bosma, M.H. Vermuë, R.H. Wijffels, Harvesting of microalgae by bio-flocculation, J. Appl. Phycol. 23 (2011) 849–855, doi:http://dx.doi.org/10.1007/s10811-010-9591-x.
[53] J. Lv, B. Guo, J. Feng, Q. Liu, F. Nan, X. Liu, S. Xie, Integration of wastewater treatment and flocculation for harvesting biomass for lipid production by a newly isolated self-flocculating microalga Scenedesmus rubescens SX, J. Clean. Prod. 240 (2019) 118211, doi:http://dx.doi.org/10.1016/j.jclepro.2019.118211.